Open Access Library Journal
2023, Volume 10, e9971
ISSN Online: 2333-9721
ISSN Print: 2333-9705

Hexagonal WO_3 Acetone Gas Sensor Modified by Graphene-COOH Functionalized (GCOOH)

Yuxuan Guo, Haiming Zhang*

School of Physical Sciences and Technology, Tiangong University, Tianjin, China
Email: *360724320@qq.com

How to cite this paper: Guo, Y.X. and Zhang, H.M. (2023) Hexagonal WO_3 Acetone Gas Sensor Modified by Graphene-COOH Functionalized (GCOOH). *Open Access Library Journal*, **10**: e9971.
https://doi.org/10.4236/oalib.1109971

Received: March 6, 2023
Accepted: March 25, 2023
Published: March 28, 2023

Abstract

GCOOH-WO_3 composites mixed with different amounts of Graphene-COOH functionalized (GCOOH) (0, 0.05, 0.1 and 0.2 wt%) were prepared by hydrothermal method at 180˚C for 10 h and 24 h. The as-prepared WO_3 and GCOOH-WO_3 composites were characterized by X-ray diffraction (XRD), scanning electron microscopy (SEM) and Raman spectroscopy and other equipment. The effect of the amount of graphene in the composites on the gas-sensing responses and the gas-sensing selectivity of the materials was investigated. The experimental results revealed that the sensor based on 0.1 wt% GCOOH-WO_3 composite exhibited high response and good selectivity to acetone at 260˚C.

Subject Areas

Physical Chemistry

Keywords

WO_3, GCOOH, Hydrothermal Method, Acetone, Gas Sensing Characteristic

1. Introduction

Volatile organic compounds (VOCs) can pollute the environment and harm human health. Acetone is one of VOCs and one of the gas in human respiration. It is used as a respiratory marker for non-invasive diagnosis of diabetes mellitus. Therefore, the detection of acetone is important for environmental safety and human health. In recent decades, many metal oxides (ZnO, In_2O_3, Fe_2O_3, SnO_2, MnO_2, Co_3O_4) have been used in sensitive studies of acetone [1] [2] [3]. Among them, WO_3 crystal, as a typical n-semiconductor, has the advantages of high cost-effectiveness, low pollution and good stability. Many experimental and theoretical results prove that WO_3 has great potential to detect VOCs in the field

of gas sensing [4] [5] [6] [7] [8].

Graphene oxide (GO) with different oxygen-containing groups such as carboxylndndnd, amino, carbonyl and other functions is extracted by gas. More adsorption sites are provided, thereby improving gas sensor sensitivity. Oxygen-containing groups in graphene oxide make it an insulating material. Graphene oxide is not a suitable gas-sensitive material because it is difficult to control the content of these groups during oxidation [9] [10] [11]. In this chapter, the effect of carboxyl (-COOH) functionalized carboxy graphene (GCOOH) on the sensing performance of WO_3 sensor is studied. Nano-composite materials with different GCOOH content, named GCOOH-WO_3, were prepared by hydrothermal method. The structure of the prepared GCOOH-WO_3 was characterized, and its gas sensitivity was tested and analyzed [12]-[19]. Therefore, this paper studies the influence of the guiding agent and graphene on the hexagonal WO_3, in order to optimize the sensing performance of the hexagonal WO_3 gas sensor, improve the response value of the hexagonal WO_3 sensor to acetone gas, reduce the operating temperature, and shorten the response and recovery time.

2. Experimental Section

Tungsten oxide GCOOH-WO_3 was synthesized by simple hydrothermal method. The preparation process is as follows: three different amounts of carboxyl-functionalized graphene were extracted from carboxyl-functionalized graphene GCOOH and dripped into deionized water for ultrasonic dispersion. Dissolve a suitable amount of sodium tungstate dihydrate in the above solution and stir for 30 minutes. Drop 6 mol·L^{-1} hydrochloric acid into the solution at a constant speed. Stir side-dropping until the pH value reaches 1.0 to 2.0. Set aside for 1 hour. Add ammonium acetate and oxalic acid to make the quality of GCOOH and WO_3 0.05 wt%, 0.1 wt%, 0.2 wt%, respectively. Stir the configured solution on a magnetic stirrer. After 3 hours of vigorous stirring, the solution turns dark blue. GCOOH-WO_3-1, GCOOH-WO_3-2, and GCOOH-WO_3-3, respectively. The milky white column powders, namely GCOOH-WO_3-1, GCOOH-WO_3-2, GCOOH-WO_3-3, were obtained by hydrothermal treatment, centrifugation and drying at 180˚C for 24 h.

3. Results and Discussion

Figure 1 shows the morphology of GCOOH-WO_3-2 composite. According to Figure 1(a) and Figure 1(b), it can be found that the columnar WO_3 is covered with graphene in flakes and agglomerates, covering the material surface, preventing the reaction with the gas to be measured, reducing the surface active sites, and affecting the reaction with the gas to be measured.

Figure 2 shows the XRD pattern of GCOOH-WO_3 composite. The main characteristic peaks are (100), (001), (110), (101), (200), (201), (220), (204). Most of the diffraction peaks of GCOOH-WO_3 can be well indexed to the XRD spectra of hexagonal tungsten trioxide WO_3 (JCPDS:00-033-1387) GCOOH-WO_3, which

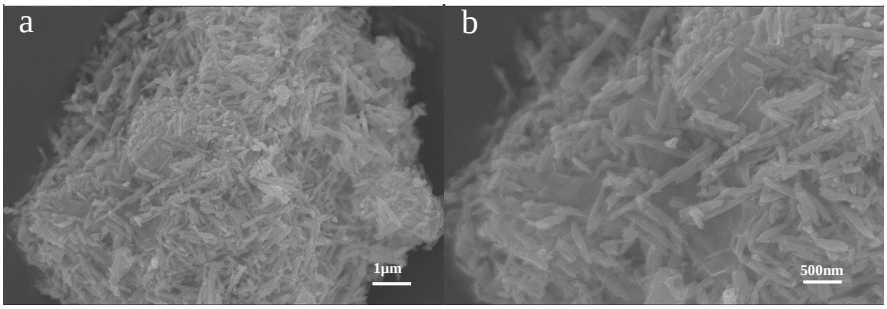

Figure 1. The SEM images of GCOOH-WO_3.

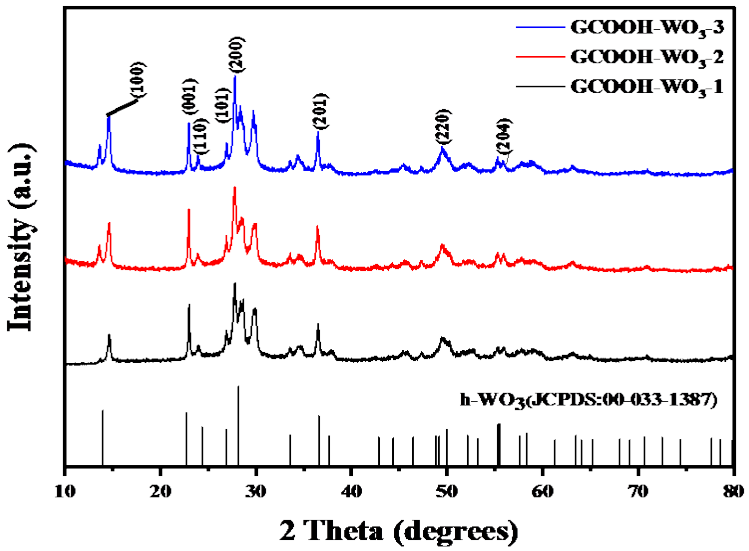

Figure 2. XRD patterns of GCOOH-WO_3.

shows that it has good crystallinity. The graphene phase cannot be detected by XRD because the modification of WO_3 nanocrystals causes the flakes of graphene to fall off.

As shown in Figure 3, GCOOH-WO_3-2 composite can detect clear peaks at 265 cm^{-1}, 704 cm^{-1} and 803 cm^{-1}. The Raman peak at 265 cm^{-1} is the stretching vibration peak of O-W-O; We can also observe two peaks at 1369 and 1620 in GCOOH-WO_3-2 complex, which are the two characteristic peaks of graphene, D and G.

Figure 4(a) shows the full spectrum of GCOOH-WO_3-2. The characteristic peaks of C1s, O1s and W4f can be observed from the figure, which proves the existence of C, O and W. Figure 4(b) shows the full spectrum of W. $W4f_{7/2}$ and $W4f_{5/2}$ represent the non-stoichiometric tungsten oxide composition at the binding energy of 35.9 eV and 54.0 eV, respectively, which further proves the formation of WO_3.

Figure 5 shows that the temperature test range is 225˚C - 325˚C, and the sensitivity of all sensors increases first and then decreases with the increase of temperature. GCOOH-WO_3-2 gas sensor has the highest sensitivity of 5.5 at 260˚C; The working state of the sensor at lower than 225˚C is not shown in the figure,

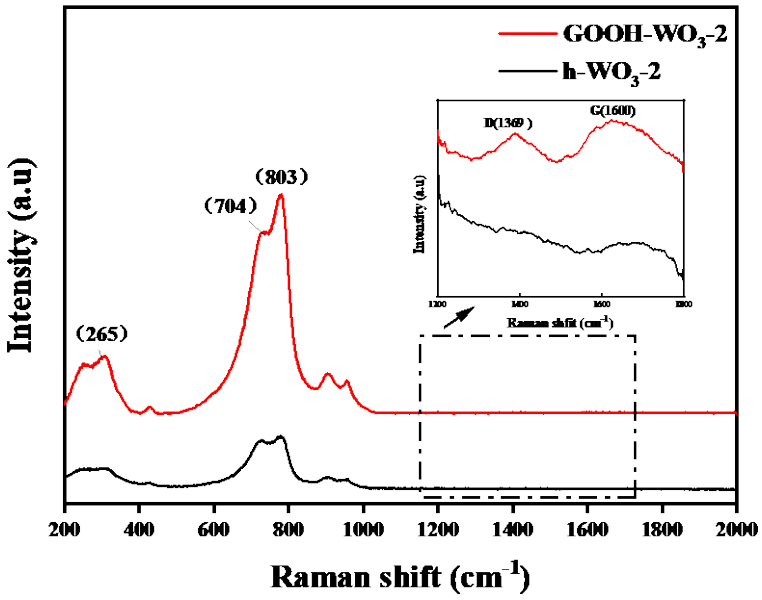

Figure 3. The Raman spectra of GCOOH-WO_3-2.

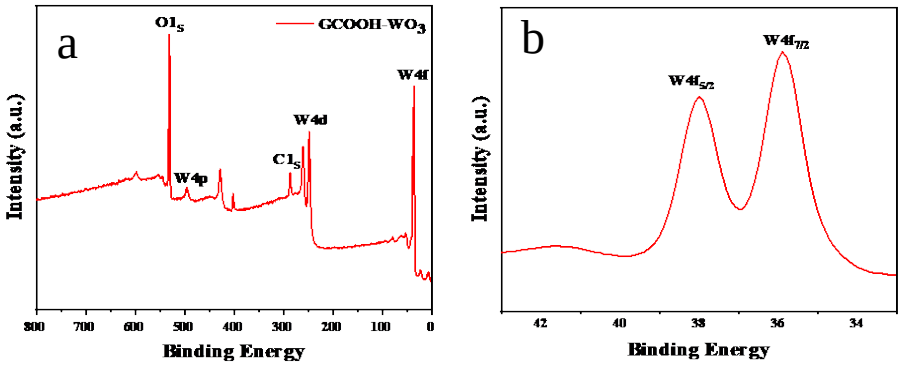

Figure 4. XPS, (a) The full spectrum of GCOOH-WO_3-2; (b) The W diagram of GCOOH-WO_3-2.

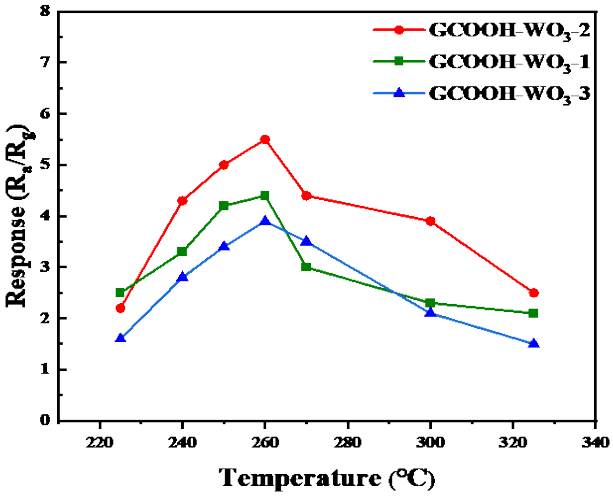

Figure 5. GCOOH-WO_3 sensitivity to different operating temperatures of 100 ppm acetone gas.

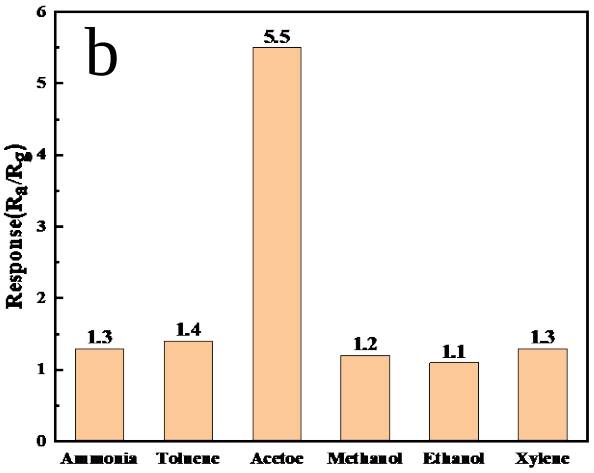

Figure 6. GCOOH-WO_3-2 100 ppm gas selectivity diagram.

because when a certain amount of GCOOH is added, the resistance of the composite material will rise, exceeding the instrument range, and can not be measured accurately at present.

The mechanism of GCOOH-WO_3 on acetone can be described as follows. When exposed to air, oxygen gets adsorbed on GCOOH-WO_3 surface, and O_2^-, O^- or O^{2-} ions will form by obtaining electrons from the conduction band, then resulting in the increased resistance. The related reactions could be expressed as Equation (1):

$$O_2(\text{gas}) \leftrightarrow O_2(\text{adsorbed}) + e^- \leftrightarrow O_2^- + e^- \leftrightarrow 2O^- \quad (1)$$

$$CH_3COCH_3 + 8O^-(\text{ads}) \rightarrow 3CO_2 + 3H_2O + 8e^- \quad (2)$$

$$CH_3COCH_3 + 6O^{2-}(\text{ads}) \rightarrow 3CO_2 + 3H_2O + 12e^- \quad (3)$$

The introduction of acetone on GCOOH-WO_3 surface will trigger the reaction with adsorbed oxygen, and meanwhile, electrons are released back to conduction band, which causing the decrease in the resistance of GCOOH-WO_3. The relevant reaction can be proposed as Equations (2)-(3). As the products (CO_2 and H_2O) desorbed from the surface, the gas sensor recovers to the initial condition. Thus, one cycle of the acetone detection is over and the sensor is ready for the next cycle (Figure 6).

4. Conclusion

In this study, GCOOH-WO_3 with different mass fractions of GCOOH was prepared by hydrothermal method. Many round graphene sheets are attached to the nanorods. GCOOH-WO_3 only responds to acetone gas. The sensing performance depends on the mass fraction of GCOOH added. It is found that only a proper amount of GCOOH can have good sensing performance.

Conflicts of Interest

The authors declare no conflicts of interest.

References

[1] Wei, S., Li, S., Wei, R., *et al.* (2021) Different Morphologies of WO_3 and Their Exposed Facets-Dependent Acetone Sensing Properties. *Sensors and Actuators B: Chemical*, **329**, Article ID: 129188. https://doi.org/10.1016/j.snb.2020.129188

[2] Mathuri, S., Margoni, M.M., Ramamurthi, K., Babu, R.R. and Ganeesh, V. (2018) Hydrothermal Assisted Growth of Vertically Aligned Platelet Like Structures of WO_3 Films on Transparent Conducting FTO Substrate for Electrochromic Performance. *Applied Surface Science*, **449**, 77-91. https://doi.org/10.1016/j.apsusc.2018.01.033

[3] Gerosa, M., Valentin, C., Onida, G., Bottani, C. and Pacchioni, G. (2016) Anisotropic Effects of Oxygen Vacancies on Electrochromic Properties and Conductivity of γ-Monoclinic WO_3. *The Journal of Physical Chemistry C*, **120**, 11716-11726. https://doi.org/10.1021/acs.jpcc.6b02707

[4] Nayak, A.K., Lee, S., Choi, Y.I., Yoon, H.J., Sohn, Y. and Pradhan, D. (2017) Crystal Phase and Size-Controlled Synthesis of Tungsten Trioxide Hydrate Nanoplates at Room Temperature: Enhanced Cr(VI) Photoreduction and Methylene Blue Adsorption Properties. *ACS Sustainable Chemistry & Engineering*, **5**, 2741-2750. https://doi.org/10.1021/acssuschemeng.6b03084

[5] Yang, H., Sun, H., Li, Q., Li, P., Song, K., Song, B. and Wang, L. (2019) Structural, Electronic, Optical and Lattice Dynamic Properties of the Different WO_3 Phases: First-Principle Calculation. *Vacuum*, **164**, 411-420. https://doi.org/10.1016/j.vacuum.2019.03.053

[6] Khadayate, R.S., Sali, J.V. and Patil, P.P. (2007) Acetone Vapor Sensing Properties of Screen Printed WO_3 Thick Films. *Talanta*, **72**, 1077-1081. https://doi.org/10.1016/j.talanta.2006.12.043

[7] Shi, J., Hu, G., Sun, Y., Geng, M., Wu, J., Liu, Y., *et al.* (2011) WO_3 Nanocrystals: Synthesis and Application in Highly Sensitive Detection of Acetone. *Sensors and Actuators B: Chemical*, **156**, 820-824. https://doi.org/10.1016/j.snb.2011.02.047

[8] Goodarzi, M.T. and Ranjbar, M. (2020) Atmospheric Flame Vapor Deposition of WO_3 Thin Films for Hydrogen Detection with Enhanced Sensing Characteristics. *Ceramics International*, **46**, 21248-21255. https://doi.org/10.1016/j.ceramint.2020.05.215

[9] Zhu, Y., Murali, S., Cai, W., Li, X., Suk, J. and Potts, J.R. (2010) Graphene and Graphene Oxide: Synthesis, Properties, and Applications. *Advanced Materials*, **22**, 3906-3924. https://doi.org/10.1002/adma.201001068

[10] Bonaccorso, F., Sun, Z., Hasan, T., and Ferrari, A. (2010) Graphene Photonics and Optoelectronics. *Nature Photonics*, **4**, 611-622. https://doi.org/10.1038/nphoton.2010.186

[11] Yi, G.-C., Wang, C. and Park, W.I. (2005) ZnO Nanorods: Synthesis, Characterization and Applications. *Semiconductor Science and Technology*, **20**, S22-S34. https://doi.org/10.1088/0268-1242/20/4/003

[12] Sun, Y., Wu, Q. and Shi, G. (2011) Graphene Based New Energy Materials. *Energy & Environmental Science*, **4**, 1113-1132. https://doi.org/10.1039/c0ee00683a

[13] Zhou, D., Cui, Y. and Han, B. (2012) Graphene-Based Hybrid Materials and Their Applications in Energy Storage and Conversion. *Chinese Science Bulletin*, **57**, 2983-2994. https://doi.org/10.1007/s11434-012-5314-9

[14] Kim, H.W., Na, H.G., Kwon, Y.J., *et al.* (2017) Microwave-Assisted Synthesis of Graphene-SnO_2 Nanocomposites and Their Applications in Gas Sensors. *ACS Ap-*

plied Materials & Interfaces, **9**, 31667-31682.
https://doi.org/10.1021/acsami.7b02533

[15] Jiang, L., Tu, S., Xue, K., Yu, H. and Hou, X. (2021) Preparation and Gas-Sensing Performance of GO/SnO_2/NiO Gas-Sensitive Composite Materials. *Ceramics International*, **47**, 7528-7538. https://doi.org/10.1016/j.ceramint.2020.10.257

[16] Li, Z., Liu, Y., Guo, D., Guo, J. and Su, Y. (2018) Room-Temperature Synthesis of CuO/Reduced Graphene Oxide Nanohybrids for High-Performance NO_2 Gas Sensor. *Sensors and Actuators B*: *Chemical*, **271**, 306-310.
https://doi.org/10.1016/j.snb.2018.05.097

[17] Karthik, P., Gowthaman, P., Venkatachalam, M. and Rajamanickam, A.T. (2020) Propose of High Performance Resistive Type H_2S and CO_2 Gas Sensing Response of Reduced Graphene Oxide/Titanium Oxide (rGO/TiO_2) Hybrid Sensors. *Journal of Materials Science*: *Materials in Electronics*, **31**, 3695-3705.
https://doi.org/10.1007/s10854-020-02928-4

[18] Zhang, H., Wang, L. and Zhang, T. (2014) Reduced Graphite Oxide/SnO_2/Au Hybrid Nanomaterials for NO_2 Sensing Performance at Relatively Low Operating Temperature. *RSC Advances*, **4**, 57436-57441. https://doi.org/10.1039/C4RA10474A

[19] Sardar, M. and Faisal, M. (2019) Methane Gas Sensor Based on Microstructured Highly Sensitive Hybrid Porous Core Photonic Crystal Fiber. *Journal of Sensor Technology*, **9**, 12-26. https://doi.org/10.4236/jst.2019.91002